

ARMY RESEARCH LABORATORY



**Single Crystal Epitaxial Germanium Based  
Ohmic Contact Structure for III-V and  
Nanoelectronic and Mesoscopic Devices**

Madan Dubey, Kenneth A. Jones, Luis M. Casas,  
Donald W. Eckart and Robert L. Pfeffer

---

ARL-TR-1122

August 1996

APPROVED FOR PUBLIC RELEASE; DISTRIBUTION IS UNLIMITED.

19960910 004

## **NOTICES**

### **Disclaimers**

**The findings in this report are not to be construed as an official Department of the Army position, unless so designated by other authorized documents.**

**The citation of trade names and names of manufacturers in this report is not to be construed as official Government endorsement or approval of commercial products or services referenced herein.**

# REPORT DOCUMENTATION PAGE

Form Approved  
OMB No. 0704-0188

Public reporting burden for this collection of information is estimated to average 1 hour per response, including the time for reviewing instructions, searching existing data sources, gathering and maintaining the data needed, and completing and reviewing the collection of information. Send comments regarding this burden estimate or any other aspect of this collection of information, including suggestions for reducing the burden, to Washington Headquarters Services, Directorate for Information Operations and Reports, 1215 Jefferson Davis Highway, Suite 1204, Arlington, VA 22202-4302, and to the Office of Management and Budget, Paperwork Reduction Project (0704-0 188), Washington, DC 20503.

|   |  |   |   |  |
|---|--|---|---|--|
| 1. AGENCY USE ONLY (Leave blank)  |  | 2. REPORT DATE<br>August 1996                           | 3. REPORT TYPE AND DATES COVERED<br>Technical Report        |  |
| 4. TITLE AND SUBTITLE<br>Single Crystal Epitaxial Germanium Based Ohmic Contact Structure For III-V and Nanoelectronic and Mesoscopic Devices   |  |   | 5. FUNDING NUMBERS  |  |
| 6. AUTHOR(S)<br>Madan Dubey, Kenneth A. Jones, Luis M. Casas, Donald W. Eckart, and Robert L. Pfeffer   |  |   |   |  |
| 7. PERFORMING ORGANIZATION NAME(S) AND ADDRESS(ES)<br>US Army Research Laboratory (ARL)<br>Physical Sciences Directorate<br>ATTN: AMSRL-PS-DB<br>Fort Monmouth, NJ 07703-5601   |  |   | 8. PERFORMING ORGANIZATION REPORT NUMBER<br><br>ARL-TR-1122 |  |
| 9. SPONSORING/MONITORING AGENCY NAME(S) AND ADDRESS(ES)   |  |   | 10. SPONSORING/MONITORING AGENCY REPORT NUMBER              |  |
| 11. SUPPLEMENTARY NOTES   |  |   |   |  |
| 12a. DISTRIBUTION/AVAILABILITY STATEMENT<br><br>Approved for public release; distribution is unlimited.   |  |   | 12b. DISTRIBUTION CODE                                      |  |
| 13. ABSTRACT (Maximum 200 words)<br><br>The single crystal epitaxial layer ohmic contacts are very promising in the fabrication of shallow junction nanoelectronic and mesoscopic devices based on III-V compounds. A single crystal Ge film is grown epitaxially on GaAs or InGaP lattice matched to GaAs and a Au or Pd layer is deposited on top of it using an Ultra High Vacuum ( $10^{-9}$ - $10^{-10}$ Torr) Electron Beam (UHV E-Beam) deposition system. The interface between the Ge and thermally cleaned GaAs or InGaP is almost atomically abrupt, smooth and oxide free, and there is a minimum of disruption of the underlying layers. When deposited at an appropriate temperature, the metals are highly oriented and have large grains. They can be diffused through the Ge film to initiate the formation on an ohmic contact in a controlled manner. A detailed analysis of interface quality, crystal structure and defect propagation in GaAs/Ge/Au, GaAs/Ge/Pd, InGaP/Ge structures is presented. High resolution Transmission Electron Microscopy (HRTEM), Double Crystal X-ray Diffraction (DXRD), Rutherford Backscattering Spectroscopy (RBS) and Auger Electron Spectroscopy (AES) were used to characterize the materials. |  |   |   |  |
| 14. SUBJECT TERMS<br><br>Single crystal, Epitaxial, Contact, Nanoelectronic, Mesoscopic   |  |   | 15. NUMBER OF PAGES<br>17                                   |  |
|   |  |   | 16. PRICE CODE  |  |
| 17. SECURITY CLASSIFICATION OF REPORT<br>Unclassified   | 18. SECURITY CLASSIFICATION OF THIS PAGE<br>Unclassified | 19. SECURITY CLASSIFICATION OF ABSTRACT<br>Unclassified | 20. LIMITATION OF ABSTRACT<br>UL                            |  |

NSN 7540-01-280-5500

Standard Form 298 (Rev. 2-89)  
Prescribed by ANSI Std. Z39-8  
298-01

**DTIC QUALITY INSPECTED 3**

## CONTENTS

|                                 | <u>Page</u> |
|---------------------------------|-------------|
| ABSTRACT .....                  | 1           |
| 1. INTRODUCTION .....           | 1           |
| 2. EXPERIMENTAL.....            | 2           |
| 3. RESULTS.....                 | 3           |
| 4. DISCUSSION .....             | 4           |
| 5. CONCLUSION AND SUMMARY ..... | 10          |
| ACKNOWLEDGEMENT .....           | 11          |
| REFERENCES.....                 | 11          |

## FIGURES

|  | <u>Page</u> |
|--|-------------|
| 1. (a) X-ray rocking curve for Au(1500 Å)/Ge(970 Å) layers on GaAs, (b) SEM micrograph of the Au surface, (c) The Auger surface chemical distribution map of the Au film of the region shown in (b).....   | 6           |
| 2. RBS channeling spectra from the Au(110) film. ....  | 6           |
| 3. XTEM micrograph of the GaAs/Ge/Au interface showing a smooth interface. ....  | 6           |
| 4. (a) HRTEM micrograph showing lattice match between GaAs/Ge, (b) AES depth profile of GaAs/Ge structure. The Ga signal for the time $t < 8.50$ min is an artifact resulting from a spectroscopic energy interference due to the presence of Ge. .... | 7           |
| 5. XTEM micrograph showing high density of dislocations in an Au film. ....  | 7           |
| 6. (a) SEM micrograph of the Pd surface. (b) X-ray diffraction pattern from the GaAs/Ge/Pd structure for which the Pd was deposited at 100°C.....  | 8           |
| 7. X-ray rocking curve for Ge on InGaP/GaAs.....   | 8           |
| 8. HRTEM micrograph of Ge/InGaP interface. ....  | 8           |

FIGURES (cont'd)

|  | <u>Page</u> |
|--|-------------|
| 9. AES depth profile of GaAs/InGaP/Ge layer. Each layer is detected clearly and the Ga signal for time $t < 4.25$ min is an artifact resulting from a spectroscopic energy interference due to the presence of Ge..... | 9           |

TABLE

|   |   |
|---|---|
| I. Reaction of Pd deposited at different temperatures on epitaxial Ge on GaAs. .... | 4 |
|---|---|

# Single Crystal Epitaxial Ge Based Ohmic Contact Structure For III-V and Nanoelectronic and Mesoscopic Devices

## ABSTRACT

The single crystal epitaxial layer ohmic contacts are very promising in the fabrication of shallow junction nanoelectronic and mesoscopic devices based on III-V compounds. A single crystal Ge film is grown epitaxially on GaAs or InGaP lattice matched to GaAs and an Au or Pd layer is deposited on top of it using an Ultra High Vacuum ( $10^{-9}$ - $10^{-10}$  Torr) Electron Beam (UHV E-Beam) deposition system. The interface between the Ge and thermally cleaned GaAs or InGaP is almost atomically abrupt, smooth and oxide free, and there is a minimum of disruption of the underlying layers. When deposited at an appropriate temperature, the metals are highly oriented and have large grains. They can be diffused through the Ge film to initiate the formation on an ohmic contact in a controlled manner. A detailed analysis of interface quality, crystal structure and defect propagation in GaAs/Ge/Au, GaAs/Ge/Pd, InGaP/Ge structures is presented. High resolution Transmission Electron Microscopy (HRTEM), Double Crystal X-ray Diffraction (DXRD), Rutherford Backscattering Spectroscopy (RBS) and Auger Electron Spectroscopy (AES) were used to characterize the materials.

## 1. INTRODUCTION

The performance of some GaAs devices is highly dependent on ohmic contacts having a smooth morphology, small contact resistance, and high reproducibility and reliability. These requirements are especially critical for dual channel high electron mobility transistors (DCHEMT's) where the device active layers are only about 50 nanometers apart, and for heterojunction bipolar transistors (HBT's) which have a thin base. The usual alloyed contact has a rough inhomogeneous interface where spiking often occurs.<sup>1</sup> One alternative is a non-alloyed contact where the contact is formed by metal-semiconductor solid state reactions.<sup>2-7</sup> The contact can be further improved by the use of single crystal epitaxial films. Such structures greatly limit grain boundary diffusion which can lead to locally deep penetration of the Ohmic metals into the semiconductor, and enable the metal, which initiates contact formation,<sup>3,6-9</sup> to come into contact with the GaAs in a controlled way by diffusing it through the epitaxial Ge layer.<sup>8,10</sup>

In addition to having similar crystal structures with a good lattice match, growth must be done under the proper deposition conditions in order to achieve good epitaxy. In the present work the experimental conditions for UHV E-Beam deposition of Ge, Pd and Au epitaxial layers on GaAs and InGaP required to form the contact structure, and characterization of the film and interface quality will be presented.

## 2. EXPERIMENTAL

The UHV E-Beam deposition system was used for all of the epitaxial growth. This system has a water-cooled main chamber with a base pressure  $1-2 \times 10^{-10}$  Torr and a load lock chamber with pressure in the range of  $10^{-7}$  Torr. The substrate can be heated from the back up to  $1000^\circ\text{C}$ . An abrupt change in the temperature is created by vertically moving the substrate away from the heater.

The GaAs substrate was cleaned in warm solvents followed by a chemical etch in an  $\text{NH}_4\text{OH} + \text{H}_2\text{O}_2 + \text{DI water}$  solution. The sample was loaded into the chamber and the temperature was raised to  $600^\circ\text{C}$  for 15 minutes to remove the native oxide on the GaAs surface. The pressure during oxide removal was in the range of mid  $10^{-8}$  Torr. The substrate temperature was reduced to  $400^\circ\text{C}$  and a Ge film 970 Å thick was deposited at a rate of 0.8-1.0 Å/sec under a pressure of  $6-9 \times 10^{-9}$  Torr. The substrate temperature was further lowered to  $100^\circ\text{C}$  and a 1500 Å gold film was deposited at a pressure of  $1-4 \times 10^{-9}$  Torr. Pd films of thickness 1000-1500 Å were also deposited on the epitaxial Ge layer at temperatures of 100, 300,  $500^\circ\text{C}$  at a deposition rate of 1-1.1 Å/sec.

In another run, a 280 Å thick InGaP film grown by OMVPE on (100) GaAs was cleaned in warm solvents and then chemically etched in a solution of  $\text{HF} + \text{HCl} + \text{DI water}$  for 1 minute before loading it into the system. The composition of InGaP was purposely selected to be slightly Ga rich so that the epitaxial Ge x-ray rocking curve peak could be distinguished from the InGaP and GaAs peaks. The wafer was heated for 5 min at  $550^\circ\text{C}$  to remove the native oxide and cooled to  $350^\circ\text{C}$  where a 600 Å thick Ge film was deposited at a rate of 0.8-1.5 Å/sec at a pressure of  $1-4 \times 10^{-9}$  Torr. The gold deposition on the Ge was the same as for the previous sample.

All the deposited films are characterized by using HRTEM, DXRD, AES, RBS, and SEM.

### 3. RESULTS

The DXRD x-ray rocking curve (Fig. 1a) of an as deposited GaAs/Ge/Au structure on the GaAs shows the peaks of GaAs(400), Ge(400), and Au(220). This suggests that the deposited Ge and Au films are epitaxial. The surface of the Au film revealed irregular dark and white patches when examined under an SEM (Fig. 1b). This surface was further analyzed by using AES which showed only the presence of Au (Fig. 1c). The crystalline quality of the Au and Ge/Au interface was also determined by RBS. Figure 2 shows the backscattering spectra of 3.02-MeV He<sup>++</sup> ions from an Au film deposited at 100°C.

The Au/Ge interface was also examined under TEM. The XTEM micrograph is shown in Fig. 3, where the GaAs/Ge and Ge/Au interfaces are smooth. A high resolution TEM (Fig. 4a) analysis of the GaAs/Ge interface showed the lattice planes of GaAs and Ge perfectly matched with no trace of an interfacial oxide layer. The AES depth profile of the GaAs/Ge film (Fig. 4b) indicates a sharp drop of the Ge concentration at the GaAs region. The Ge/Au interface (Fig. 5) showed an average density of  $8 \times 10^5 \text{ cm}^{-2}$  threading dislocations originating at the interface and passing through the Au film to the surface perpendicular to the interface. Two large grains of Au with a sharp grain boundary are also visible in the micrograph in which dislocations are crossing. The electron diffraction pattern of the Ge/Au film has an orientation relation of (110)Au || (001)Ge and [001]Au || [110]Ge.<sup>11</sup>

The GaAs/Ge structures, in which Pd was deposited on epitaxial Ge at different temperatures, were analyzed by x-ray diffraction, and the results are summarized in Table 1. The x-ray diffraction curve for the Pd film deposited at 100°C is shown in Fig. 6b and a smooth surface feature is observed in the SEM micrograph (Fig. 6a).

In the GaAs/InGaP/Ge structure, the Ge was epitaxial to the InGaP, as analyzed by DXRD (Fig. 7). A smooth (001) InGaP/Ge interface is visible under lattice resolution XTEM (Fig. 8). A sharp change in the Ge concentration is also observed in the InGaP region in the AES depth profile of the GaAs/InGaP/Ge structure (Fig. 9).

TABLE I. Reaction of Pd deposited at different temperatures on epitaxial Ge on GaAs.

| Temperature of Pd deposition (°C) | Pd/(1,000 Å)<br>Pd epitaxy<br>d(Å) <i>hkl</i> | on Ge(1,000 Å)<br>Ge-Pd<br>d(Å) <i>hkl</i>            | on GaAs<br>Pd-Ga-As<br>d(Å) <i>hkl</i>   |
|-----------------------------------|---|---|--|
| 100                               | 2.23 (111)                                    |   |  |
| 300                               |   | 2.67 (111)<br>2.15 (211)<br>2.09 (121)<br>1.335 (041) |  |
| 500                               |   | 2.66 (111)<br>2.08 (121)<br>1.47 (212)                | 3.44 (110)<br>2.83 (111)<br>2.44 (002)<br>2.18 (002)<br>1.99 (211)<br>1.47 (311) |

#### 4. DISCUSSION

The GaAs/Ge/Au interface (Fig. 3) is smooth and Ge and Au are crystalline (Figs. 1,4a, 5). The in-situ oxide cleaning of GaAs using ion sputtering has shown improvement in ohmic contacts.<sup>12</sup> However the surface damage due to ion interaction is still a major concern for the reliability of contacts. The thermal cleaning of the oxide on GaAs in a UHV system leaves a smooth surface (roughness less than 10 Å). Figure 4a shows a continuous Ge lattice fringe along the GaAs surface with no trace of an oxide (i.e., amorphous region).

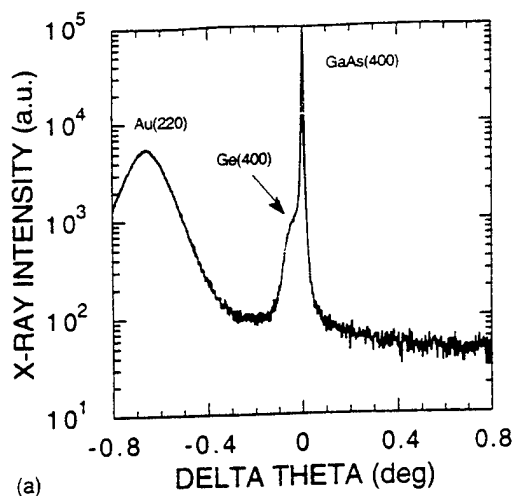
The reaction of Au/Ge at 100°C was not detectable in XTEM, RBS and AES. The AES analysis of the Au surface does not reveal any Ge contamination (Fig. 1c). It is interesting to mention<sup>13</sup> that the volume diffusion coefficient of Ge in Au at room temperature is very small, but the extrapolated value of the grain boundary diffusion coefficient of Ge in Au is about  $10^{-16}$  cm<sup>2</sup>/sec at 30°C. The present Au film has very large grains (more than 1μm), therefore the probability of Au grain boundary diffusion even at 100°C is very small.

The sharp channeling curve (Fig. 2) is also indicative of a highly oriented Au film. The  $c_{\min}$ =axial minimum yield=minimum of the ratio between the channeled and random spectrum, which occurs between 450 and 480 MeV in Figure 2, is  $c_{\min}$  =2.97%. This suggests the Au film is single crystal or is highly oriented with large crystals. For a random network,  $c_{\min}$  is 100%, and for perfect single crystals, theory predicts that  $c_{\min}$  is on the order of a few percent.

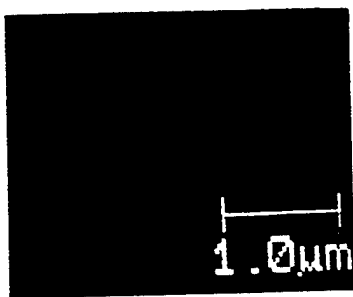
The diffusion of Ge into GaAs is also minimum as shown in the AES depth profile (Fig 4b). Therefore, the Ge does not appear to diffuse into the GaAs to form an ohmic contact; it must await the in-diffusion of the top metal to the Ge-GaAs interface to facilitate the process. This can be done in a controlled way by an annealing process.

The reaction of Pd with Ge at 100°C is minimal as is seen by the weak x-ray diffraction peaks of a Pd-Ge phase (Fig. 6b). The strong peaks of Ge(400) and GaAs(400) are due to a single crystal structure formation while the Pd (111) peak may be due to a single crystal or highly oriented (111) Pd grains in the thin film. The x-ray diffraction of Pd films deposited at 300°C and 500°C showed peaks corresponding to Ge-Pd and Ge-Pd-Ga phases, respectively (Table 1). The shiny Pd surface of the film grown at 100°C (Fig. 6a) is also indicative of a Pd film that has reacted only slightly with the Ge.

The InGaP/Ge interface (Fig. 8) was also smooth and Ge was crystalline as it was for the growth on GaAs. The AES depth profile (Fig. 9) revealed an abrupt change of Ge concentration in the InGaP region and thus a minimum diffusion of the Ge into the InGaP layer. This is a major step towards the goal of getting an abrupt and smooth metal contact for the shallow junction III-V device. The Au or Pd on top of the Ge was also the same as mentioned above. Therefore, a UHV E-Beam system can deposit epitaxial Ge and Au on oxide free GaAs and InGaP without using an As or P gas over pressure. The roughness of the surface was less than 10 Å, and epitaxial deposition of Ge at 400°C and Au or Pd at 100°C does not show any visible interdiffusion.



(a)



(b)



(c)

FIG. 1. (a) X-ray rocking curve for Au(1500 Å)/Ge(970 Å) layers on GaAs, (b) SEM micrograph of the Au surface, (c) The Auger surface chemical distribution map of the Au film of the region shown in (b).

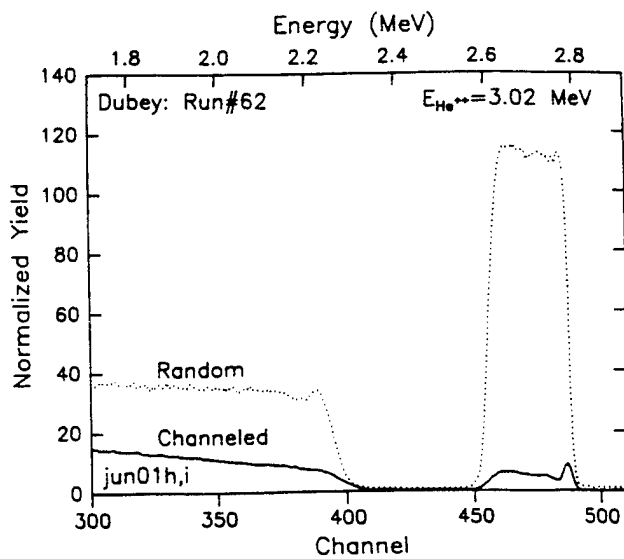


FIG. 2. RBS channeling spectra from the Au(110) film.

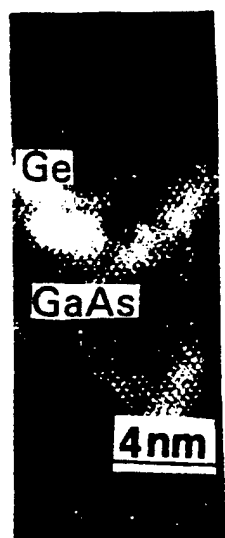


50 nm

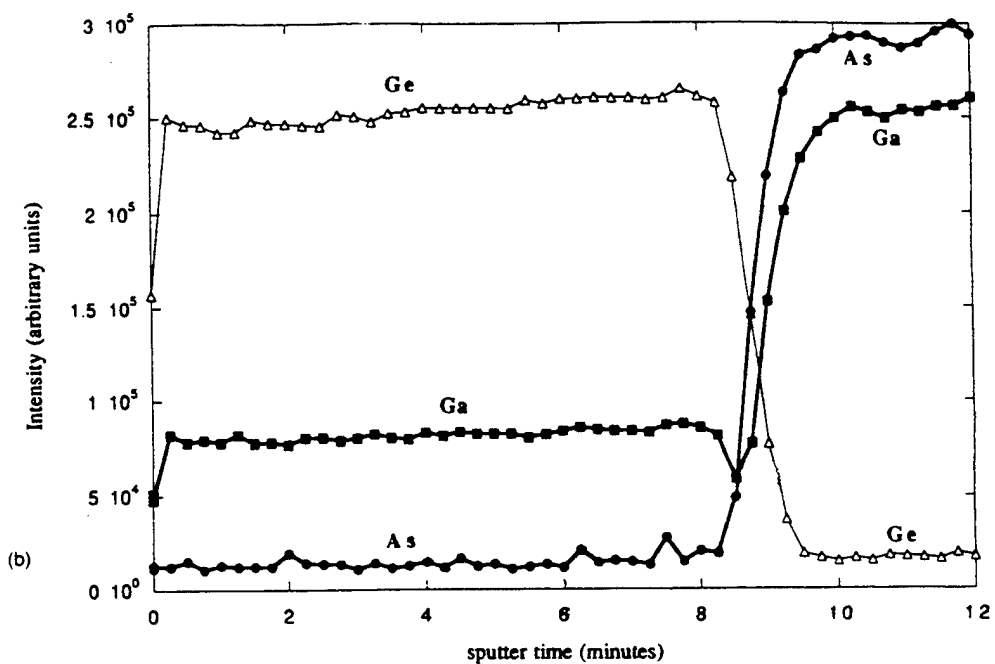
Ge

GaAs

FIG. 3. XTEM micrograph of the GaAs/Ge/Au interface showing a smooth interface.

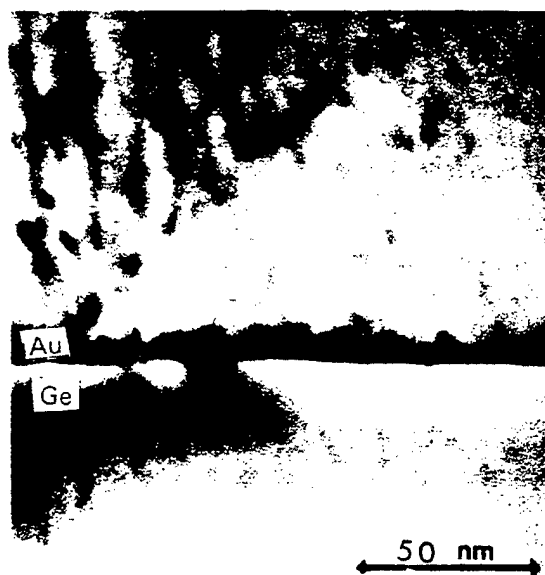


(a)



(b)

FIG. 4. (a) HRTEM micrograph showing lattice match between GaAs/Ge. (b) AES depth profile of GaAs/Ge structure. The Ga signal for the time  $t < 8.50$  min is an artifact resulting from a spectroscopic energy interference due to the presence of Ge.



GaAs

FIG. 5. XTEM micrograph showing high density of dislocations in an Au film.

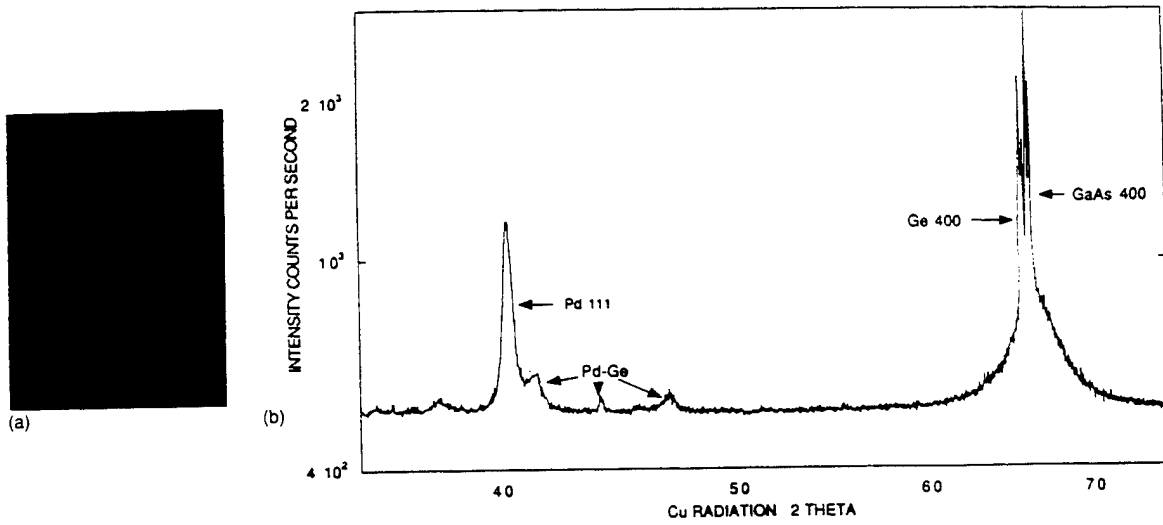


FIG. 6. (a) SEM micrograph of the Pd surface. (b) X-ray diffraction pattern from the GaAs/Ge/Pd structure for which the Pd was deposited at 100°C.

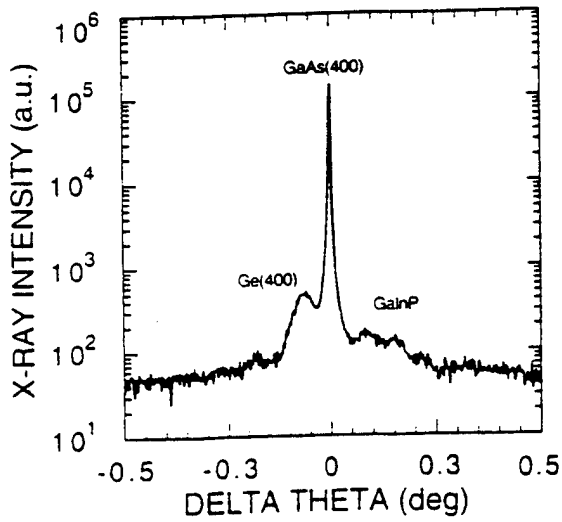


FIG. 7. X-ray rocking curve for Ge on InGaP/GaAs.

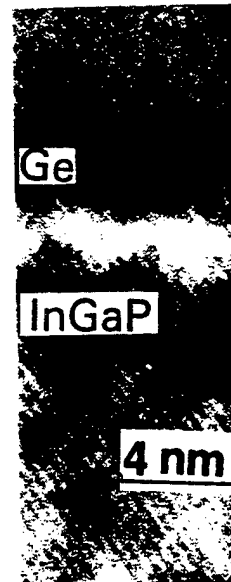


FIG. 8. HRTEM micrograph of Ge/InGaP interface.

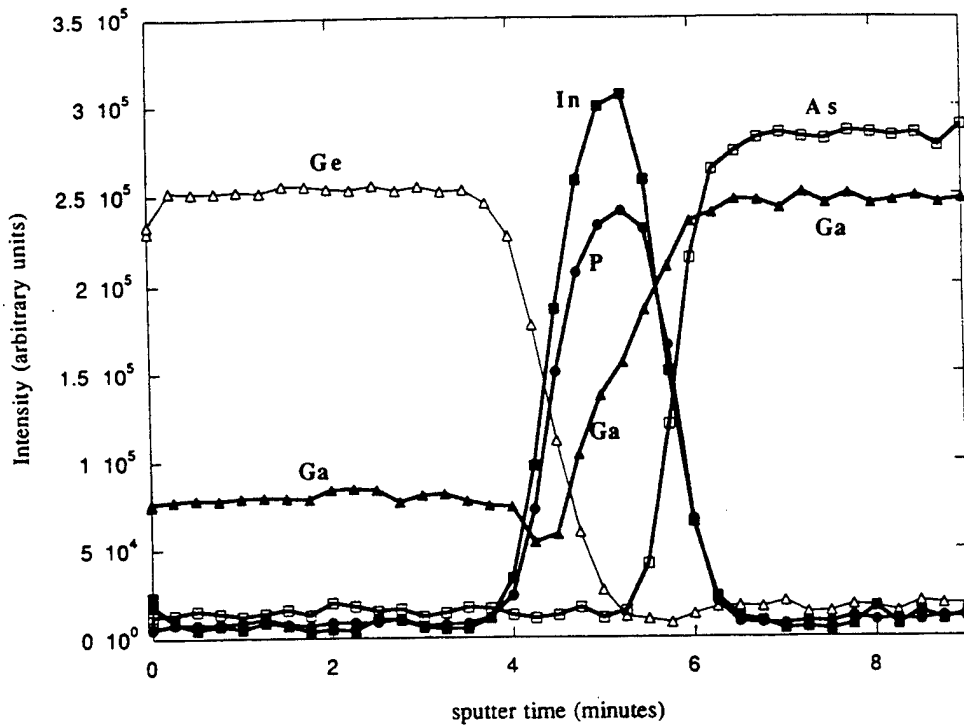


FIG. 9. AES depth profile of GaAs/InGaP/Ge layer. Each layer is detected clearly and the Ga signal for time  $t < 4.25$  min is an artifact resulting from a spectroscopic energy interference due to the presence of Ge.

## 5. CONCLUSION AND SUMMARY

Ultra-smooth Ge-GaAs or InGaP and Ge-Au or Pd interfaces without the presence of any oxide layer can be obtained using a UHV E-Beam deposition system. The present method does not require any As or P gas over pressure while cleaning the GaAs or InGaP surface. The single crystal Ge and large, highly oriented polycrystal metal layers will minimize the grain boundary diffusion process. A highly oriented or single crystal Au or Pd layer can be deposited on the Ge with only a minimal reaction with it by selecting a suitable deposition temperature. The metal can then be diffused through the single crystal Ge film to react with the GaAs and initiate ohmic contact formation in a controlled manner.

## ACKNOWLEDGMENT

The authors wish to thank Dr. Joe Flemish for assistance in the DXRD studies.

## REFERENCES

1. N. Braslau, *Thin Solid Films*. 104, 391 (1983).
2. O. Aina, W. Katz, B.J. Baliga, and K. Rose, *J. Appl. Phys.* 53, 777 (1982).
3. M.S. Dornath-Mohr, M.W. Cole, H.S. Lee, D.C. Fox, D.W. Eckart, R.T. Lareau, W.H. Chang and K.A. Jones, *J. Electronic Mat.* 19, 1247 (1990).
4. E.D. Marshall, W.X. Chen, C.S. Wu and T.F. Kuech. *Appl. Phys. Lett.* 47, 298 (1985).
5. C.J. Palmstrom, S.A. Schwarz, E. Yablonovitch, J.P. Harbison, C.L. Schwartz, L.T. Florez, T.J. Gmitter, E.D. Marshall and S.S. Lau, *J. Appl. Phys.* 67, 334 (1990).
6. W.Y. Han, H.S. Lee, Y. Lu, M.W. Cole, L.M. Casas, A. DeAnni, K.A. Jones, and L.W. Yang, *J. Appl. Phys.* 74, 754 (1993).
7. M.W. Cole, W.Y. Han, L.M. Casas, D.W. Eckart and K.A. Jones, *J. Vac. Sci. Tech.* 12A, 1904, 1994.
8. H. Lee, K.A. Jones, M.W. Cole, R.T. Lareau, S.N. Schauer, W. Vavra and R. Clarke, *J. Appl. Phys.* 72, 4773 (1992).
9. J.T. Lai and J.Y. Lee, *J. Appl. Phys.* 76, 1686 (1994).
10. W.J. Devlin, C.E.C. Wood, R. Stall, and L.F. Eastman, *Soild State Electronics*. 23, 823 (1980).
11. M. Dubey, K.A. Jones, D.W. Eckart, L.M. Casas, and R.L. Pfeffer. *Appl. Phys. Lett* 64, 2697 (1994).
12. F. Ren, S.J. Pearton, T.R. Fullowan, W.S. Hobson, S.N.G. Chu, and A.B. Emerson in *Advanced III-V Compound Semiconductor Growth, Processing and Devices*, edited by S.J. Pearton, D.K. Sadana, and J.M. Zavda (*Mater. Res. Soc. Proc.* 240, Pittsburgh, PA, 1992) pp. 417-424.
13. T. Kim, and D.D.L. Chung, *J. Vacuum Sci. Technol.* B4, 762 (1986).

ARMY RESEARCH LABORATORY  
PHYSICAL SCIENCES DIRECTORATE  
MANDATORY DISTRIBUTION LIST

August 1996  
Page 1 of 2

Defense Technical Information Center\*  
ATTN: DTIC-OCC  
8725 John J. Kingman Rd STE 0944  
Fort Belvoir, VA 22060-6218  
(\*Note: Two DTIC copies will be sent  
from STINFO office, Ft. Monmouth, NJ)

- Director  
US Army Material Systems Analysis Actv  
ATTN: DRXSY-MP  
(1) Aberdeen Proving Ground, MD 21005

- Commander, AMC  
ATTN: AMCDE-SC  
5001 Eisenhower Ave.  
(1) Alexandria, VA 22333-0001

- Director  
Army Research Laboratory  
ATTN: AMSRL-D (John W. Lyons)  
2800 Powder Mill Road  
(1) Adelphi, MD 20783-1197

- Director  
Army Research Laboratory  
ATTN: AMSRL-DD (COL Thomas A. Dunn)  
2800 Powder Mill Road  
(1) Adelphi, MD 20783-1197

- Director  
Army Research Laboratory  
2800 Powder Mill Road  
Adelphi, MD 20783-1197  
(1) AMSRL-OP-SD-TA (ARL Records Mgt)  
(1) AMSRL-OP-SD-TL (ARL Tech Library)  
(1) AMSRL-OP-SD-TP (ARL Tech Publ Br)

- Directorate Executive  
Army Research Laboratory  
Physical Sciences Directorate  
Fort Monmouth, NJ 07703-5601  
(1) AMSRL-PS-A (V. Rosati)  
(1) AMSRL-PS-T (M. Hayes)  
(22) Originating Office

- Advisory Group on Electron Devices  
ATTN: Documents  
Crystal Square 4  
1745 Jefferson Davis Highway, Suite 500  
(2) Arlington, VA 22202

- Commander, CECOM  
R&D Technical Library  
Fort Monmouth, NJ 07703-5703  
(1) AMSEL-IM-BM-I-L-R (Tech Library)  
(3) AMSEL-IM-BM-I-L-R (STINFO Ofc)

ARMY RESEARCH LABORATORY  
PHYSICAL SCIENCES DIRECTORATE  
SUPPLEMENTAL DISTRIBUTION LIST  
(ELECTIVE)

August 1996  
Page 2 of 2

- Deputy for Science & Technology  
Office, Asst Sec Army (R&D)  
(1) Washington, DC 20310
- Cdr. Marine Corps Liaison Office  
ATTN: AMSEL-LN-MC  
(1) Fort Monmouth, NJ 07703-5033
- HQDA (DAMA-ARZ-D/  
Dr. F.D. Verderame)  
(1) Washington, DC 20310
- Director  
Naval Research Laboratory  
ATTN: Code 2627  
(1) Washington, DC 20375-5000
- USAF Rome Laboratory  
Technical Library, FL2810  
ATTN: Documents Library  
Corridor W, STE 262, RL/SUL  
26 Electronics Parkway, Bldg. 106  
Griffiss Air Force Base  
(1) NY 13441-4514
- Dir, ARL Battlefield  
Environment Directorate  
ATTN: AMSRL-BE  
White Sands Missile Range  
(1) NM 88002-5501
- Dir, ARL Sensors, Signatures,  
Signal & Information Processing  
Directorate (S3I)  
ATTN: AMSRL-SS  
2800 Powder Mill Road  
(1) Adelphi, MD 20783-1197
- Dir, CECOM Night Vision/  
Electronic Sensors Directorate  
ATTN: AMSEL-RD-NV-D  
(1) Fort Belvoir, VA 22060-5806
- Dir, CECOM Intelligence and  
Electronic Warfare Directorate  
ATTN: AMSEL-RD-IEW-D  
Vint Hill Farms Station  
(1) Warrenton, VA 22186-5100